Coupled Systems Mechanics, *Vol. 9, No. 2 (2020) 163-182*
DOI: https://doi.org/10.12989/csm.2020.9.2.163

Thermo-mechanical analysis of reinforced concrete slab using different fire models

Samir Suljevic*[1,2], Senad Medic[1a] and Mustafa Hrasnica[1b]

[1]Faculty of Civil Engineering, University of Sarajevo, Patriotske lige 30, 71000 Sarajevo, Bosnia and Herzegovina
[2]Université de Technologie de Compiègne/Sorbonne Universités, Laboratoire Roberval de Mécanique, Centre de Recherche Royallieu, 60200 Compiègne, France

(Received January 4, 2020, Revised January 28, 2020, Accepted February 8, 2020)

Abstract. Coupled thermo-mechanical analysis of reinforced concrete slab at elevated temperatures from a fire accounting for nonlinear thermal parameters is carried out. The main focus of the paper is put on a one-way continuous reinforced concrete slab exposed to fire from the single (bottom) side as the most typical working condition under fire loading. Although contemporary techniques alongside the fire protection measures are in constant development, in most cases it is not possible to avoid the material deterioration particularly nearby the exposed surface from a fire. Thereby the structural fire resistance of reinforced concrete slabs is mostly influenced by a relative distance between reinforcement and the exposed surface. A parametric study with variable concrete cover ranging from 15 mm to 35 mm is performed. As the first part of a one-way coupled thermo-mechanical analysis, transient nonlinear heat transfer analysis is performed by applying the net heat flux on the exposed surface. The solution of proposed heat analysis is obtained at certain time steps of interest by α-method using the explicit Euler time-integration scheme. Spatial discretization is done by the finite element method using a 1D 2-noded truss element with the temperature nodal values as unknowns. The obtained results in terms of temperature field inside the element are compared with available numerical and experimental results. A high level of agreement can be observed, implying the proposed model capable of describing the temperature field during a fire. Accompanying thermal analysis, mechanical analysis is performed in two ways. Firstly, using the guidelines given in Eurocode 2 - Part 1-2 resulting in the fire resistance rating for the aforementioned concrete cover values. The second way is a fully numerical coupled analysis carried out in general-purpose finite element software DIANA FEA. Both approaches indicate structural fire behavior similar to those observed in large-scale fire tests.

Keywords: Thermo-mechanical analysis, reinforced concrete slab, fire loads, standard ISO 834 fire curve, parametric fire curves, structural fire resistance

1. Introduction

Due to highly complex physical phenomena typically presented in concrete structures exposed to elevated temperatures (Ibrahimbegovic *et al.* 2010, Huang 2010), properly evaluating both fire resistance rating and response have become a more challenging task over the last few decades.

*Corresponding author, Ph.D. Student, E-mail: samir.suljevic@gf.unsa.ba, samir.suljevic@utc.fr
[a]Assistant Profesor, E-mail: senad_medic@yahoo.com
[b]Full Professor, E-mail: hrasnica@bih.net.ba

http://www.techno-press.org/?journal=csm&subpage=8 ISSN: 2234-2184 (Print), 2234-2192 (Online)

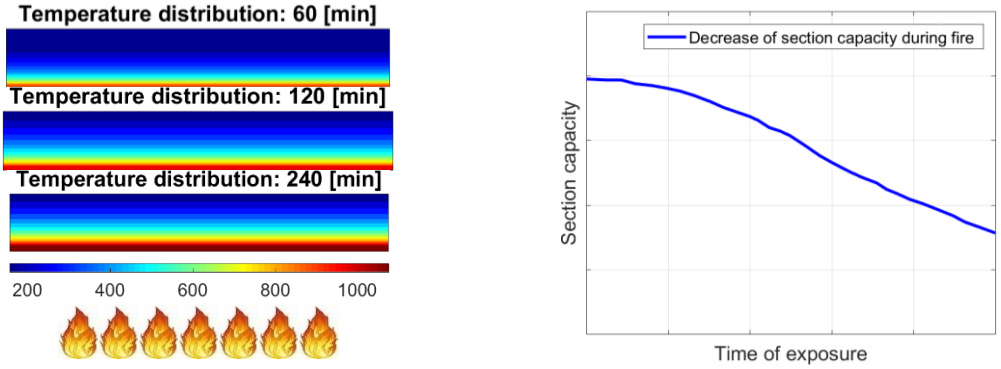

Fig. 1 Deterioration of material properties due to high temperatures leads to reducing section capacity

Furthermore, recent developments in computational technology have enabled capturing most of these effects appropriately using numerical models, as performed in Ngo *et al.* (2014) and Ngo *et al.* (2013). However, many questions and uncertainties related to these effects are still open.

Most building codes recognize the importance of structural fire analysis which becomes the essential requirement alongside the standard requirements closely related to capacity demand for the standard static and dynamic loads applied on a structure. In this regard, buildings must meet certain criteria commonly related to the type of occupancy and height of structures in order to obtain proper fire resistance rating. However, special treatment in terms of fire protection should be implemented on a huge majority of buildings built earlier without considering the fire resistance.

This paper deals with the assessment of the structural fire rating of a one-way continuous reinforced concrete (RC) slab. Generally, RC slabs are the most sensitive structural elements exposed to the fire load (Guo and Shi 2011). Consequently, special attention should be denoted to design them properly.

According to the temperature field for certain time periods shown in Fig. 1, temperatures at exposed surface exceed 1000ºC. Significant decrease of yield strength of reinforcing steel starts from 500ºC, which gradually leads to decreasing of the structural capacity of a critical section (Ngo *et al.* 2014). Furthermore, the concrete in upper layers is practically unaffected making the relative distance of reinforcement to exposed surface a crucial feature in achieving the satisfactory fire resistance rating.

In this study, different heating regimes are indirectly taken modeling the fire using both standard ISO 834 temperature-time curve and parametric temperature-time curves. Parametric temperature-time curves are obtained assuming a concrete fire compartment with various opening factors and differently controlled burning during the post-flashover fire.

2. Thermal analysis

The first step in the process of calculating structural fire rating is to carry out a thermal analysis. In this example, thermal analysis is done using own developed software accounting for nonlinear thermal characteristics of concrete and in the finite element package DIANA FEA. According to Bangash (2010), the contribution of reinforcement on the temperature field inside the reinforced concrete sections is not significant and in most cases could be neglected. This assumption is applied

in further analysis.

The simplest way accounting for thermal analysis is the use of tabulated data or temperature profiles given in the literature (Eurocode 2 2004, Guo and Shi 2011). The approach presented in this paper utilizes FEM procedures for solving transient nonlinear heat transfer, whereas temperature profiles are used as a benchmark in order to validate the results of the analysis.

Thermal characteristics of concrete are taken from Eurocode 2. A lower limit for thermal conductivity and specific heat corresponding to dry concrete (u=0%) are assumed. Temperature-dependent thermal conductivity, density, and specific heat are shown in Fig. 2 and Fig. 3.

Regarding the fire model, standard ISO 834 temperature-time curve is defined by the logarithmic expression (Eurocode 1 2002)

$$\theta_g = 345 \cdot log(8t + 1) + 20 \tag{1}$$

where θ_g is the gas temperature in [°C] and t is the time of exposure in minutes. As already mentioned, single-sided exposure is considered.

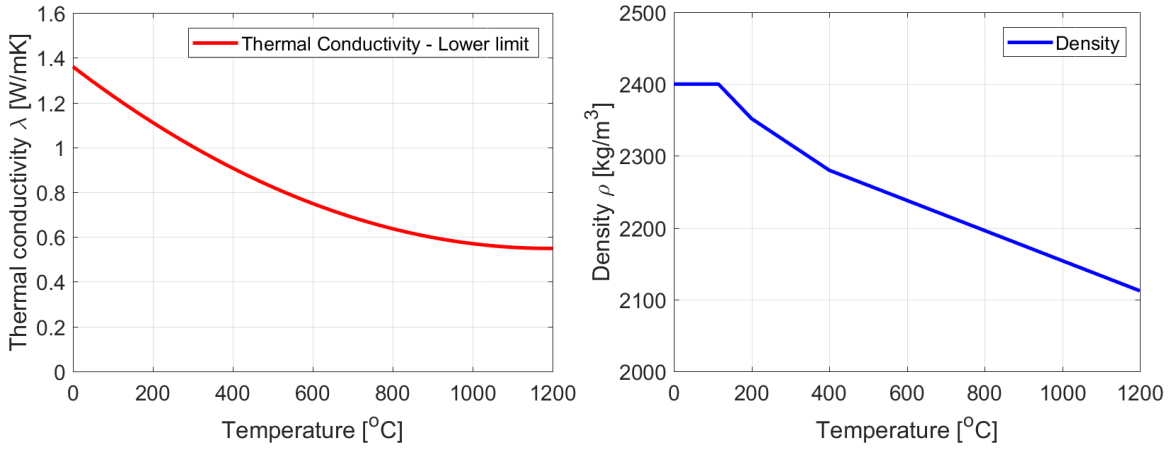

(a) (b)

Fig. 2 Thermal characteristics of concrete: (a) Thermal conductivity (b) Concrete density

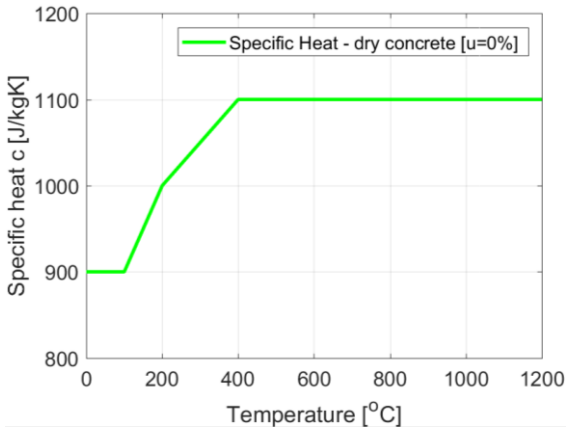

Fig. 3 Specific heat of concrete with respect to temperature

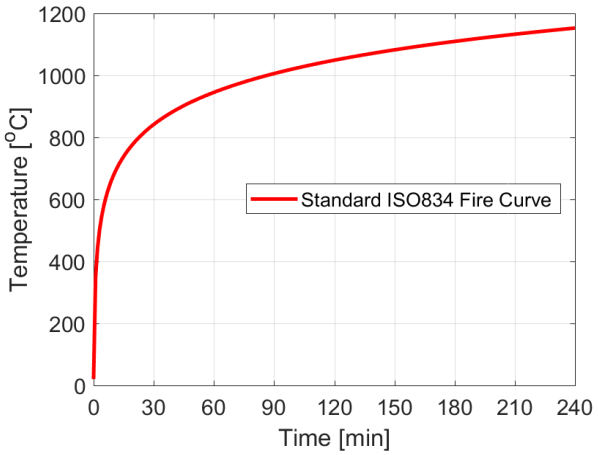

Fig. 4 Standard ISO 834 temperature-time curve

Transient heat transfer is defined by a well-known parabolic partial differential equation

$$\frac{\partial\theta}{\partial t} - \alpha \cdot \frac{\partial^2\theta}{\partial x^2} = 0 \ , \ \alpha = \frac{\lambda}{c \cdot \rho}, \tag{2}$$

where λ is thermal conductivity, c is specific heat, ρ is density and α is thermal diffusivity.

Modeling the temperature development in case of fire request existing all mechanisms of heat transfer: conduction, convection and radiation. Conduction is used to describe the heat flow through the solid media, while convection and radiation are responsible for net heat flux applied on a boundary surface in terms of Robin's boundary condition.

These mechanisms are governed by the following equations

$$h_x = -\lambda \cdot \frac{d\theta}{dx} \tag{3}$$

$$h_{net} = h_{net,c} + h_{net,r} \ \Rightarrow \ \left[h_{net,c} = h \cdot (\theta_g - \theta_s),\ h_{net,r} = \varepsilon \cdot \sigma \cdot (\theta_r^4 - \theta_s^4) \right] \tag{4}$$

Eq. (3) is a well-known Fourier's law, which closely links the temperature gradients and the heat fluxes whereas thermal conductivity λ is a proportionality factor. Equation (4) represents net heat flux consisted of both a convection term and a radiation term. In the upper equation, h is a convection coefficient (assumed $h_x = 25 \frac{W}{m^2 K}$), θ_s is ambient temperature, ε=0.8is emissivity and σ is Steffan-Boltzmann constant equal to $\sigma = 5.67 \cdot 10^{-8} \frac{\mathrm{W}}{\mathrm{m^2 K^4}}$.

Spatial discretization is performed using 1D 2-noded truss elements with the temperature nodal values as unknowns. The latter element is capable of describing linear temperature field and constant heat flux across the element.

Discretizing the partial differential equation which describes transient heat transfer results in the following matrix equation (Wickström 2016)

$$[M] \cdot \{\dot{\theta}\} + [K] \cdot \{\theta\} = \{F\} \tag{5}$$

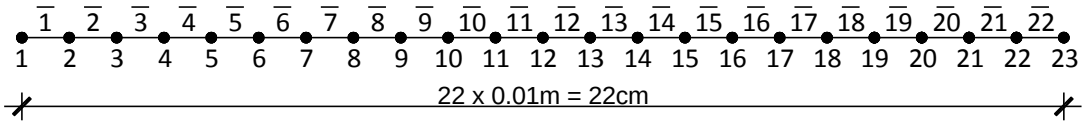

Fig. 5 Spatial discretization using 1D 2-noded finite elements

Table 1 Temperature of the exposed slab surface

Time step [min]	Temperature [˚C]	Time step [min]	Temperature [˚C]
30	765.16	120	1024.20
60	902.58	180	1091.42
90	974.99	240	1138.01

where $[M]$ is the global mass matrix, $[K]$ is the global thermal conductivity matrix, $\{\theta\}$ is the vector of nodal temperatures, the vector $\{\dot{\theta}\}$ contains time derivatives of nodal temperatures, and $\{F\}$ is the vector of net heat flow.

Numerical time integration is performed using the so-called α-method, proposed in Ibrahimbegovic (2009) and Logan (2011). The parameter α can be interpreted as a measure of the degree of implicitness. Using α=0, which corresponds to an explicit (forward Euler) time integration scheme and with substitution

$$\left\{\dot{\theta}\right\} \approx \frac{\Delta\{\theta\}}{\Delta t} = \frac{\{\theta\}^{j+1} - \{\theta\}^{j}}{\Delta t} \tag{6}$$

related to small time step, Eq. (6) yields a more convenient form

$$\frac{1}{\Delta t} \cdot [M] \cdot \{\theta\}^{j+1} = \left(\frac{1}{\Delta t} \cdot [M] - [K] \right) \cdot \{\theta\}^{j} + \{F\}^{j} \tag{7}$$

Since the temperature distribution in j-th time step is known, explicit relation for temperature distribution at (j+1)-th time step can be written as

$$\{\theta\}^{j+1} = \{\theta\}^{j} + \Delta t \cdot [M]^{-1} \cdot \left(\{F\}^{j} - [K] \cdot \{\theta\}^{j} \right) \tag{8}$$

The explicit time integration scheme is conditionally stable (Ghaboussi and Wu 2017, Ibrahimbegovic 2009) with constrained put on time step length. In order to ensure stability condition, as a precondition to ensure convergence of the method, time step length has to be smaller than the critical time step. For the proposed model, critical time step length is

$$\Delta t_{cr} = \frac{\rho \cdot c \cdot \Delta x^2}{\lambda + h / \Delta x} \tag{9}$$

The time step length used in the analysis is Δt=2s, thereby ensuring stability condition and convergence of the method.

Results of nonlinear transient heat transfer are shown in Table 1. and Fig. 8. The Fig. 8 demonstrates well agreement between temperature field proposed in this model and one specified in Eurocode 2 in terms of temperature profiles for similar thermal characteristics. The main

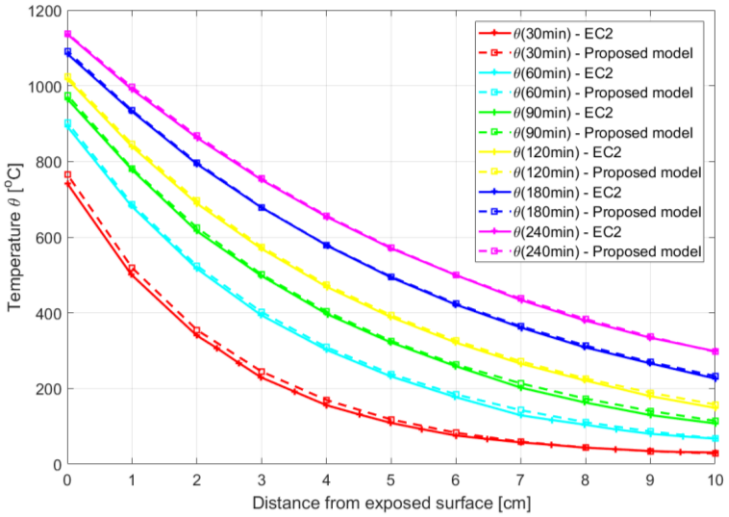

Fig. 6 Graphical interpretation of transient nonlinear heat transfer analysis

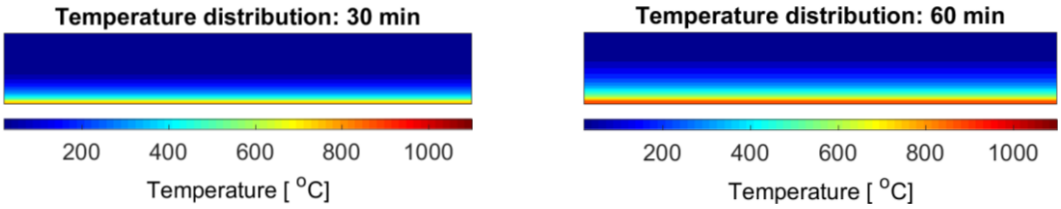

Fig. 7 Temperature rise after 30 min (left) and 60 min (right) exposure to standard fire curve

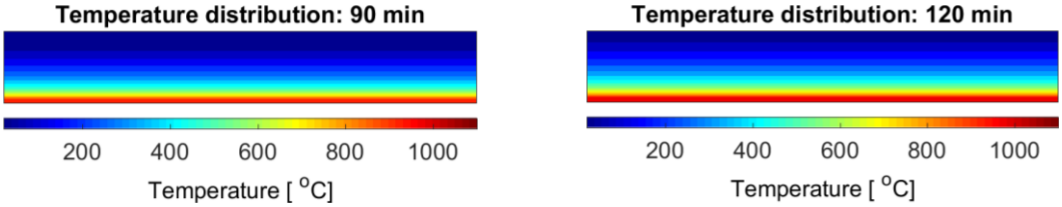

Fig. 8 Temperature rise after 90 min (left) and 120 min (right) exposure to standard fire curve

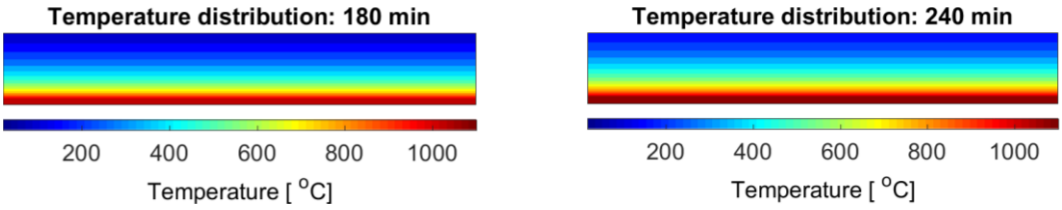

Fig. 9 Temperature rise after 180 min (left) and 240 min (right) exposure to standard fire curve

difference is that the Eurocode temperature profiles are given for 20 cm-thick slab, while in this example slab with a height of 22 cm is analyzed.

This temperature field is consistent with the results of Wickström's method (Purkiss and Li 2014) based on a superposition of simple solutions to the Fourier heat transfer equation. Assuming the

same thermal characteristics, this approach leads to the following graphical results in certain time steps:

Actually, it may be concluded that Wickström's method slightly overestimates the temperature rise at both the early stage of fire development and in the fully developed fire. However, since the temperatures values for all three methods proposed here are within 30°C of each other, any of these approaches can be used in determination temperature distribution inside the cross-section assuming standard fire exposure. These results are in agreement with the previous researches (Sangluaia *et al.* 2013, Allam *et al.* 2013, Balaji *et al.* 2016, Suljevic *et al.* 2019)

In order to determine the behavior of RC slabs during the different heating regimes, parametric temperature-time curves are used. Thereby the descending branch is included, which is neglected in case of standard ISO 834 curve. Generally, parametric fire curves could be applied only to post-flashover fires, assuming uniform temperature inside the compartment. Post-flashover fires can be either ventilation controlled or fuel controlled. In the first case, the rate of combustion depends on the size and shape of vertical openings, while the second one is controlled by the surface area of the fuel (Buchanan and Abu 2017).

In that sense, we analyzed several different fire scenarios described by both ventilation controlled and fuel controlled fire. Ventilation areas are introduced by specifying the values of opening factors O. In this example, values of 0.05 $m^{1/2}$ and O=0.10 $m^{1/2}$ are chosen.

The geometrical and thermal characteristics of the compartment alongside the data related to the intensity of fire load are shown in Table 2.

Parametric curves are obtained following the procedure in Eurocode 1-Part 1-2 (Annex A).

Thermal analysis is performed for three different values of concrete cover: 15 mm, 25 mm, 35 mm. The results of nonlinear thermal analysis, in the form of temperatures in reinforcement, are shown in Fig. 13-Fig. 20.

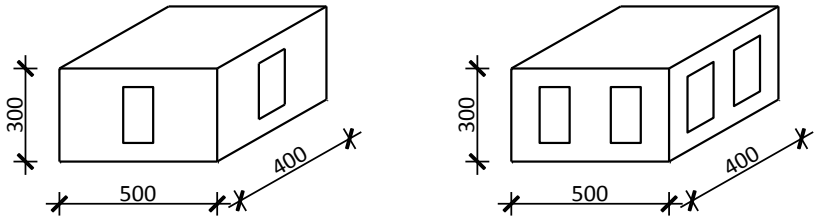

Fig. 10 Fire compartments with opening factors O=0.05 $m^{1/2}$ and O=0.10 $m^{1/2}$

Table 2 Fire compartment data

Compartment dimensions (L/B/H) in [m]	5 m/4 m/3 m
Area of vertical openings in [m^2]	3.5 m^2 (O=0.05 $m^{1/2}$) and 7.0 m^2 (O=0.10 $m^{1/2}$)
Characteristics of compartment linings	Concrete: 1. Specific heat capacity: $c = 1000$ J/kgK 2. Thermal conductivity: $\lambda = 1.5$ W/mK 3. Density: $\rho = 2400$ kg/m^3
Characteristic fire load density [MJ/m^2]	Type of occupancy: Office $q_f = 500$ MJ/m^2 (fractile 80%)
Rate of fire growth	Slow, Medium and Fast

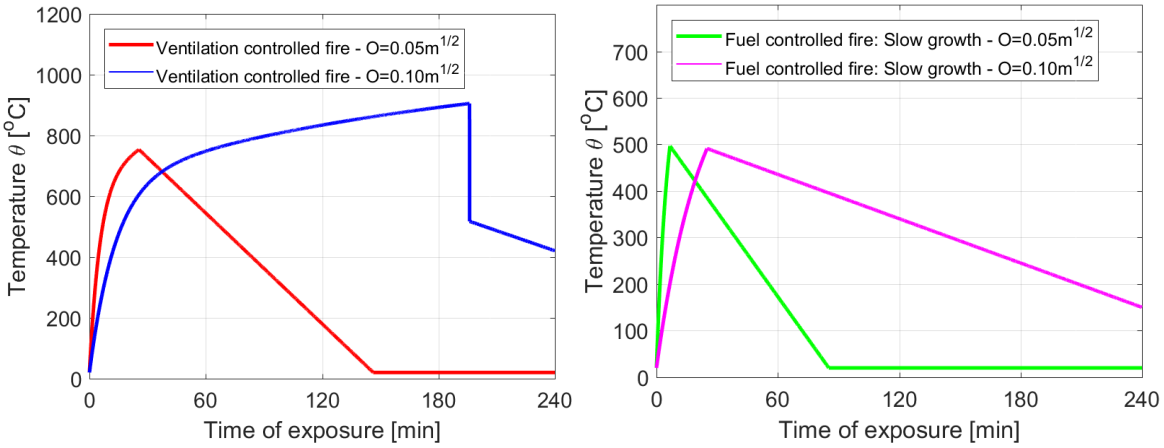

Fig. 11 Parametric fire curves for ventilation and fuel controlled fire with slow fire growth

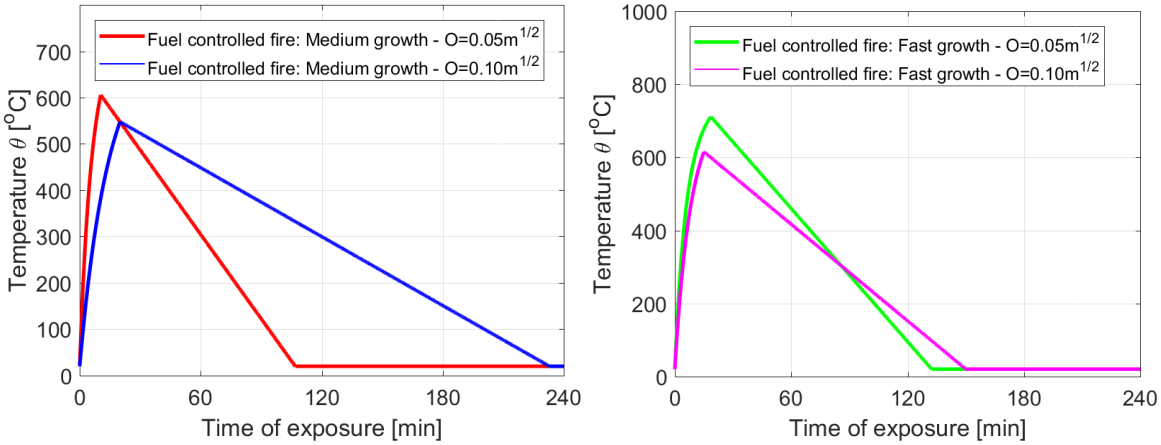

Fig. 12 Parametric fire curves for fuel controlled fires with medium (left) and fast fire growth (right)

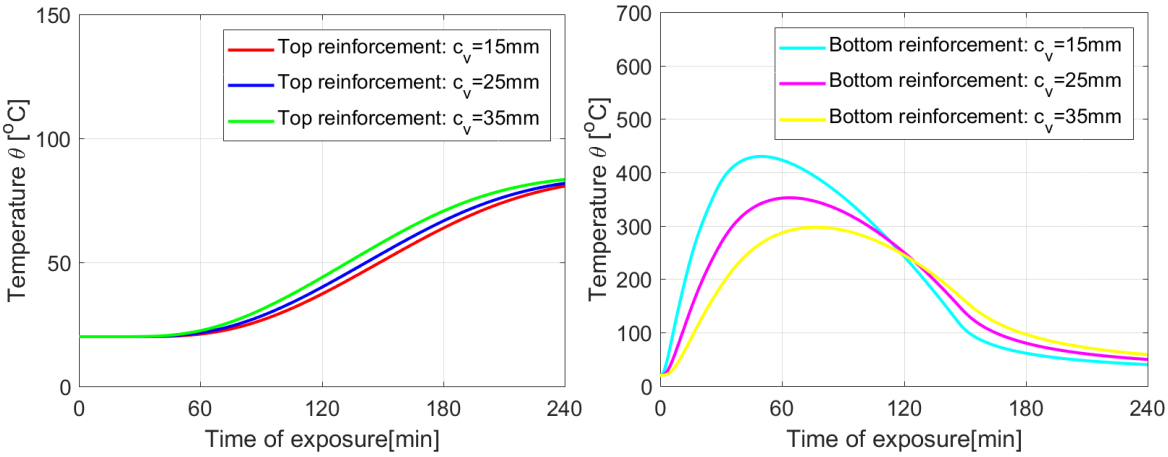

Fig. 13 Temperatures in reinforcement: Ventilation controlled fire with O=0.05 m$^{1/2}$

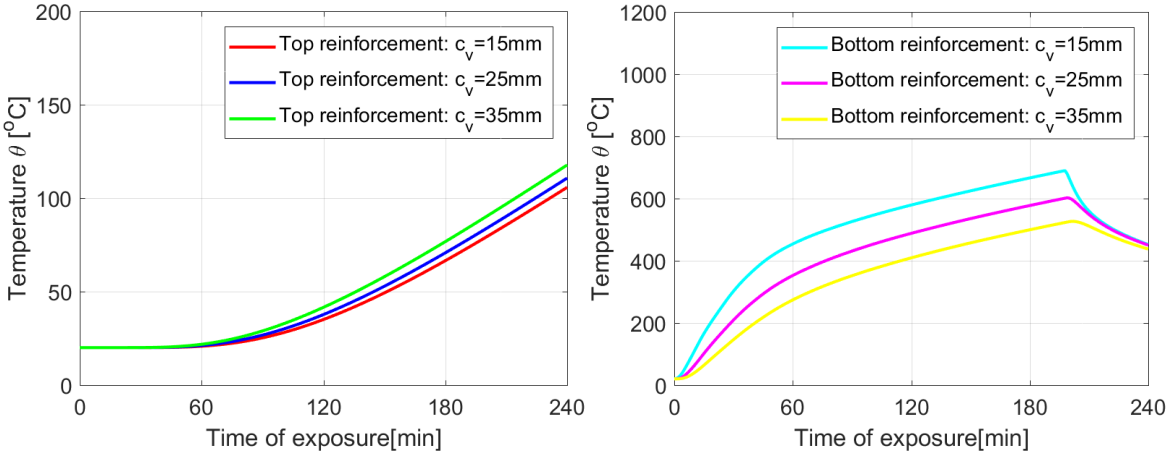

Fig. 14 Temperatures in reinforcement: Ventilation controlled fire with O=0.10 m$^{1/2}$

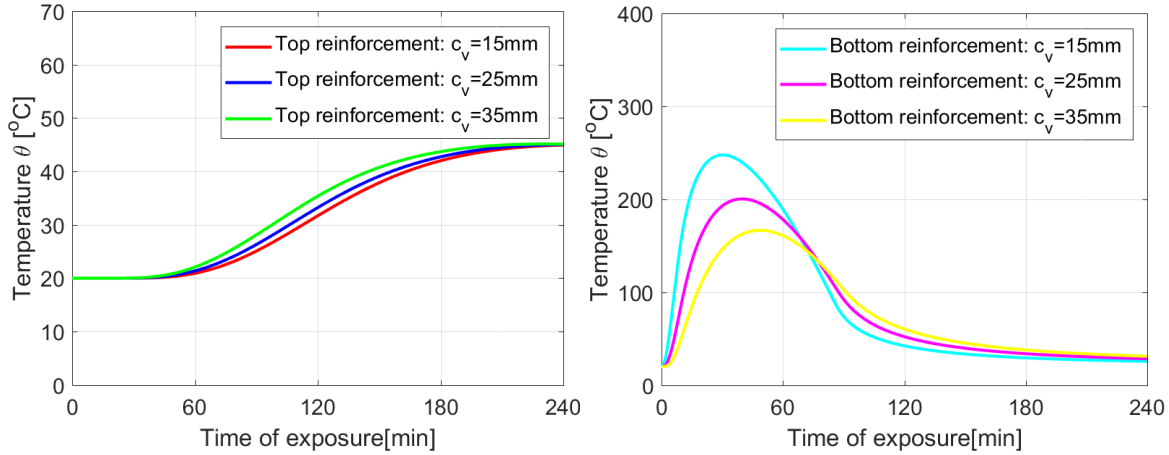

Fig. 15 Temperatures in reinforcement: Fuel controlled fire - Slow fire growth: O=0.05 m$^{1/2}$

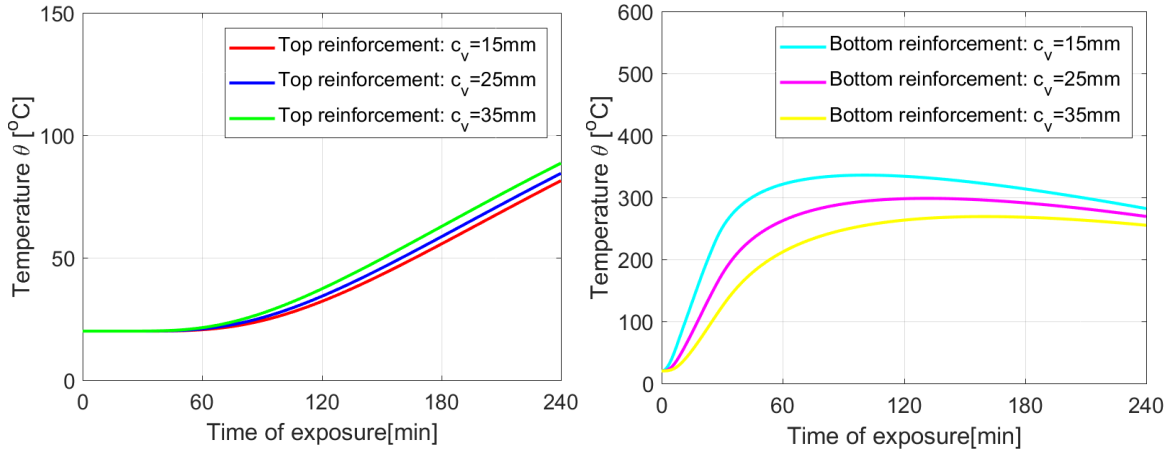

Fig. 16 Temperatures in reinforcement: Fuel controlled fire - Slow fire growth: O=0.10 m$^{1/2}$

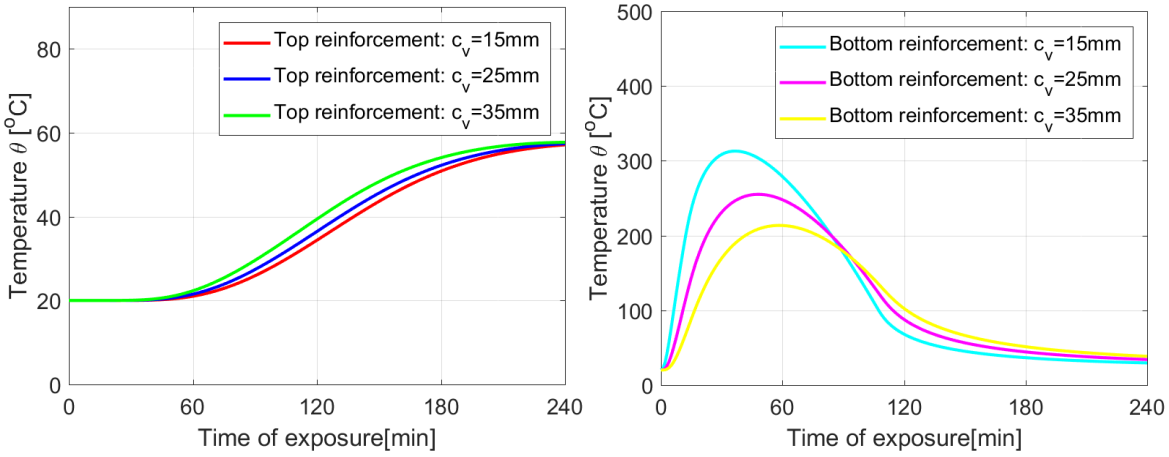

Fig. 17 Temperatures in reinforcement: Fuel controlled fire - Medium fire growth: O=0.05 m$^{1/2}$

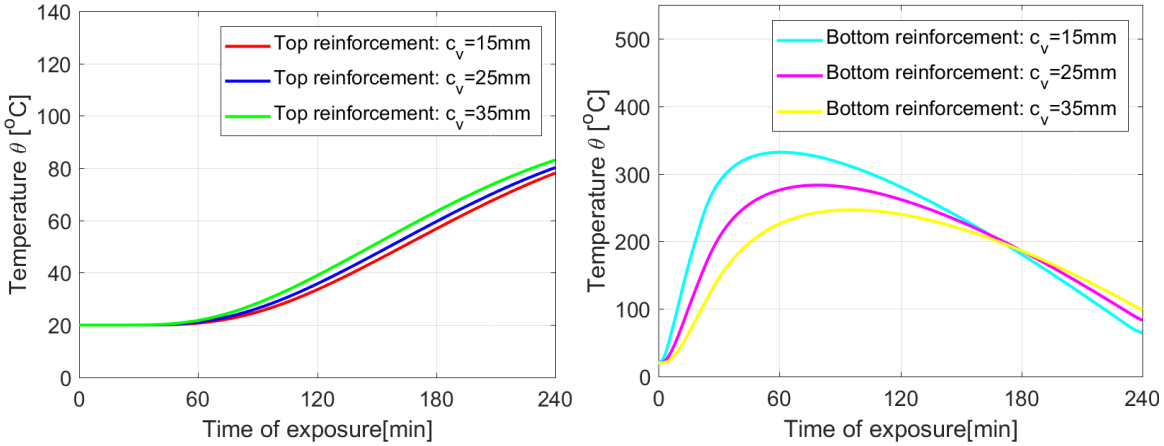

Fig. 18 Temperatures in reinforcement: Fuel controlled fire - Medium fire growth: O=0.10 m$^{1/2}$

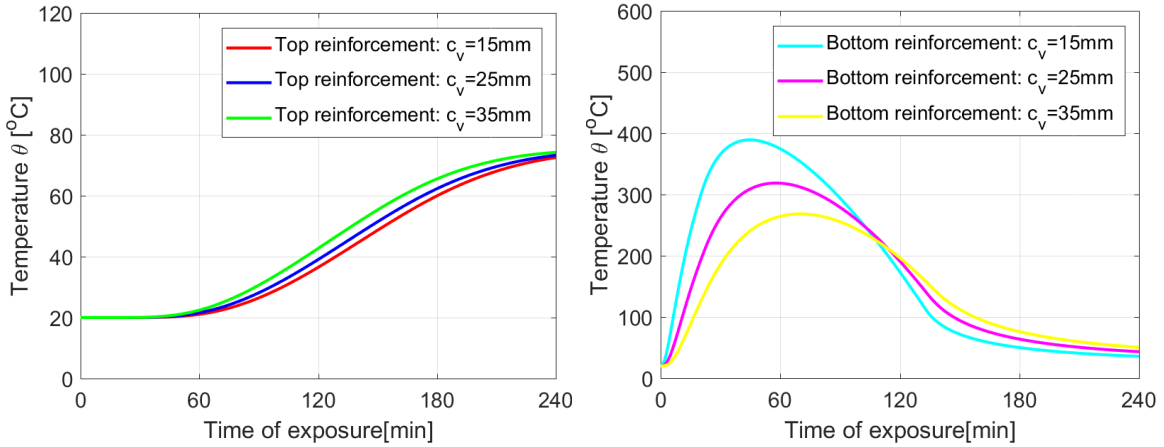

Fig. 19 Temperatures in reinforcement: Fuel controlled fire - Fast fire growth: O=0.05 m$^{1/2}$

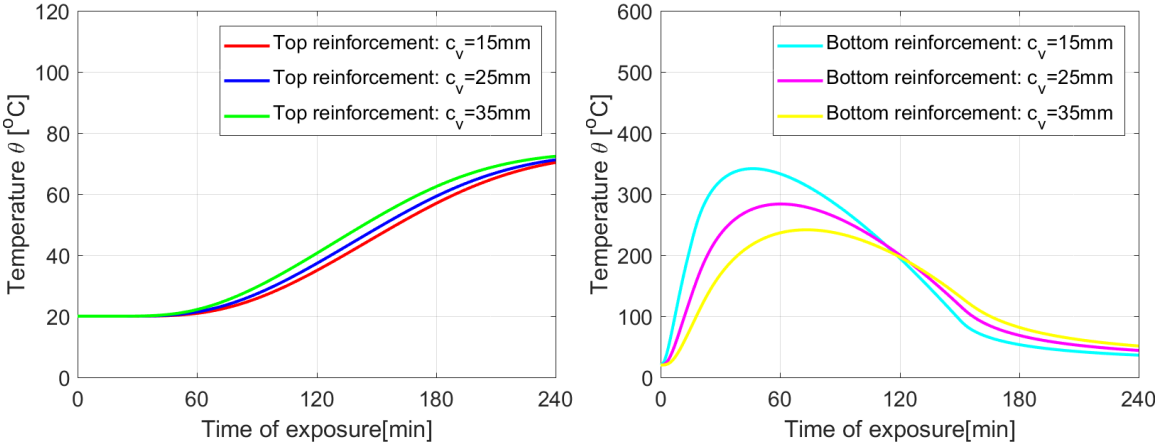

Fig. 20 Temperatures in reinforcement: Fuel controlled fire - Fast fire growth: O=0.10 m$^{1/2}$

In the case of ventilation controlled fire (O=0.05 m$^{1/2}$), early temperature descent approximately started after 30 min of fire exposure causes nonlinear time-dependent temperature distribution in both top and bottom reinforcement layers, graphically displayed by temperature curves corresponding to appropriate concrete cover. Furthermore, this heating regime causes overlapping of latter curves at the intersection point of 120 min in terms of time. Despite the fire temperature drops off at an early stage of fire development, an expected change of the temperature field inside the section is postponed for the next 90 minutes. That is due to the significant thermal inertia of concrete along with increasing specific heat and decreasing thermal conductivity during the fire.

However, previously observed interference of curves describing the temperature in bottom reinforcement during the heating regime is no longer possible for the upper reinforcement.

Regardless of the fire model, the temperature rise in upper reinforcement layers starts just before the 60 minutes of fire exposure.

Generally, increasing the concrete cover contributes greatly to reducing the risk of reaching yield stress in bottom reinforcement. This is the most common sign of failure accompanied by the crushing of concrete in the compressive zone (Guo and Shi 2011).

3. Mechanical analysis

After performing the thermal analysis, mechanical analysis is the last step which is aimed at the determination of structural fire resistance. Commonly, structural fire resistance is defined as a time in which structural members elapsed before a fire limit is violated. Naturally, the resistance in whatever way defined is mostly dependent on the mechanical properties of constituent materials.

In application to structural fire resistance, it is necessary to analyze the temperature-dependent mechanical properties of materials. This directly associates the utmost importance of reinforcement position inside the RC section. Since the resultant force in reinforcement directly influences the arm of internal forces inside the section, it means the structural fire capacity of the RC slab is time (or temperature) dependent unlike the calculation approach in ambient temperatures.

In this paper, mechanical analysis is carried out on the RC slab with a thickness of 22 cm. The slab is made of concrete C25/30 with characteristic compressive strength f_{ck}=25 N/mm^2 and

reinforcement B500S in the form of welded ribbed mesh with characteristic yield strength: f_{yk}=500 N/mm^2.

Load transfer is assumed only in the longitudinal direction of the structural member, implying the width of the slab equal to 100 cm. Longitudinal thermal deformation is neglected since it is assumed that the slab is restrained by beams and columns.

For the purpose of internal force computation, Eurocode 2 allows to analyze continuous slab as a simply supported slab if redistribution of bending moments at normal temperature design exceeds 15%. Redistribution of moments is preferred because it exploits ductility and allows the forming of plastic hinges near supports. Therefore internal forces are calculated on a simply supported slab.

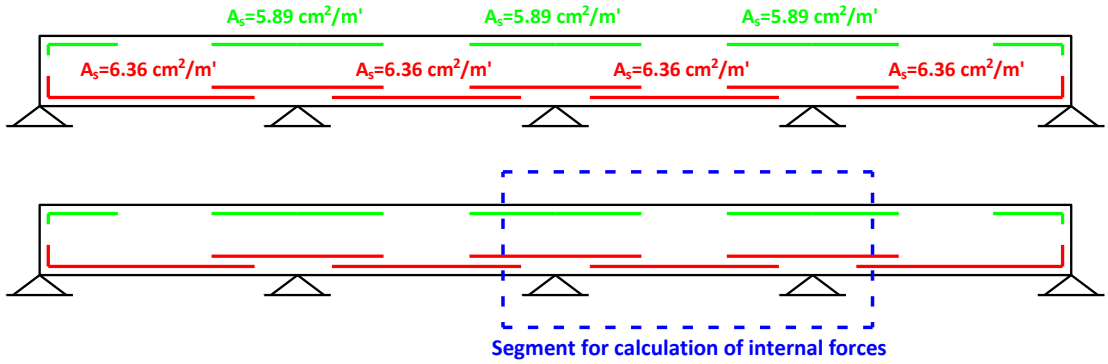

Fig. 21 Calculation model for the mechanical part of structural fire analysis

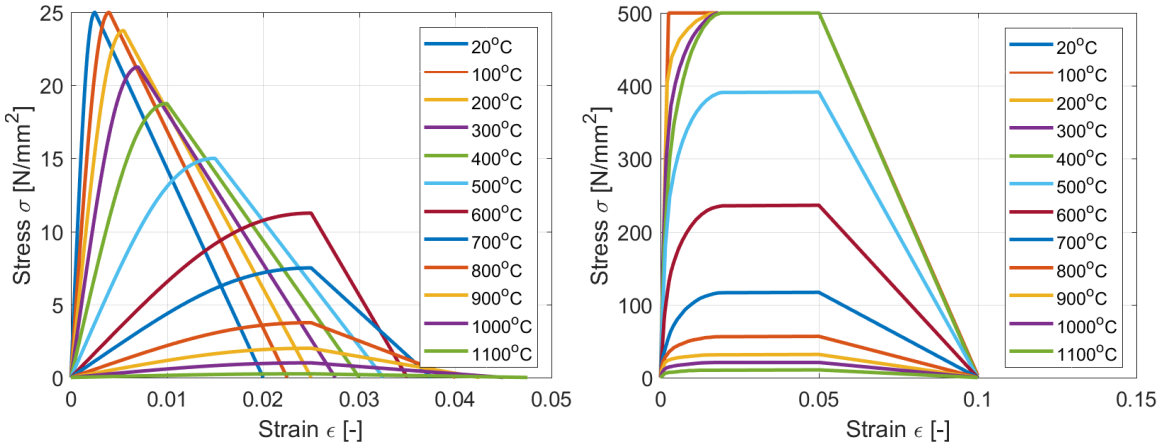

Fig. 22 Stress-strain relationship for concrete (left) and reinforcement (right) at elevated temperatures

A parametric study with variable values of concrete cover ranging from 15mm to 35mm along with modeling fire using standard ISO 834 fire curve and parametric fire curves is carried out. The stress-strain relationships for concrete and reinforcement accounting for thermal-dependent strengths of both materials, according to Eurocode 2, are shown below:

The resistance of critical cross-section is obtained using 500°C isotherm method assuming equivalent rectangular compression stress block in concrete, while design loads are calculated for

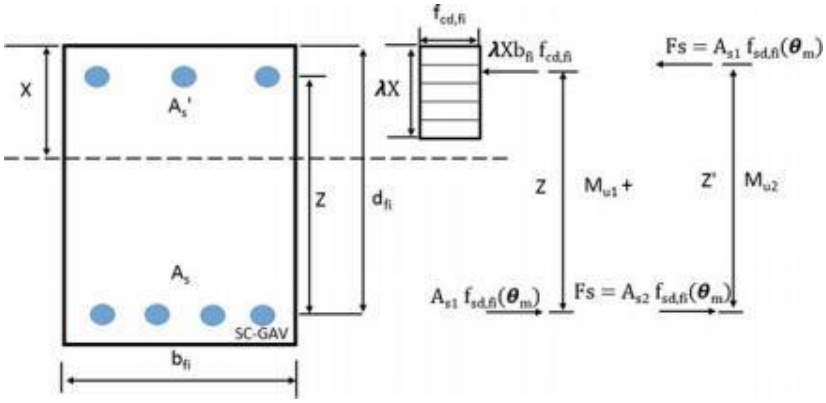

Fig. 23 Stress distribution at ultimate limit state for a rectangular cross-section with compression reinforcement (Eurocode 2 2004, Chandrasekaran and Srivastava 2018)

Table 3 Structural fire resistance (concrete cover: c_v=15 mm)-Fire model: Standard ISO 834

Time t [min]	T_{fire} [°C]	T_{steel} [°C]	F_{steel} [kN]	x [m]	$\lambda \cdot x$ [m]	d-0,5·$\lambda \cdot x$ [m]	$M_{Rd,fi}$ [kNm/m]
30	841.8	303.2	318.0	0.016	0.013	0.200	63.58
60	945.3	470.4	254.4	0.013	0.010	0.200	50.87
90	1006.0	571.2	178.1	0.009	0.007	0.200	35.54
120	1049.0	642.9	117.7	0.006	0.005	0.200	23.53
180	1109.7	743.7	57.2	0.003	0.002	0.200	11.45
240	1152.8	815.0	35.0	0.002	0.001	0.200	7.00

Table 4 Structural fire resistance (concrete cover: c_v=25 mm)-Fire model: Standard ISO 834

Time t [min]	T_{fire} [°C]	T_{steel} [°C]	F_{steel} [kN]	x [m]	$\lambda \cdot x$ [m]	d-0,5·$\lambda \cdot x$ [m]	$M_{Rd,fi}$ [kNm/m]
30	841.8	209.3	318.0	0.016	0.013	0.190	60.40
60	945.3	360.7	318.0	0.016	0.013	0.190	60.40
90	1006.0	458.7	260.8	0.013	0.010	0.190	49.46
120	1049.0	530.7	216.2	0.011	0.009	0.190	41.08
180	1109.7	634.4	124.0	0.006	0.005	0.190	23.56
240	1152.8	709.3	70.0	0.003	0.003	0.190	13.29

Table 5 Structural fire resistance (concrete cover: c_v=35 mm)-Fire model: Standard ISO 834

Time t [min]	T_{fire} [˚C]	T_{steel} [˚C]	F_{steel} [kN]	x [m]	$\lambda \cdot x$ [m]	d-0,5·$\lambda \cdot x$ [m]	$M_{Rd,fi}$ [kNm/m]
30	841.8	144.9	318.0	0.016	0.013	0.180	57.22
60	945.3	277.6	318.0	0.016	0.013	0.180	57.22
90	1006.0	369.5	318.0	0.016	0.013	0.180	57.15
120	1049.0	439.2	267.1	0.013	0.011	0.180	48.07
180	1109.7	542.0	206.7	0.010	0.008	0.180	37.20
240	1152.8	618.0	136.7	0.007	0.005	0.180	24.61

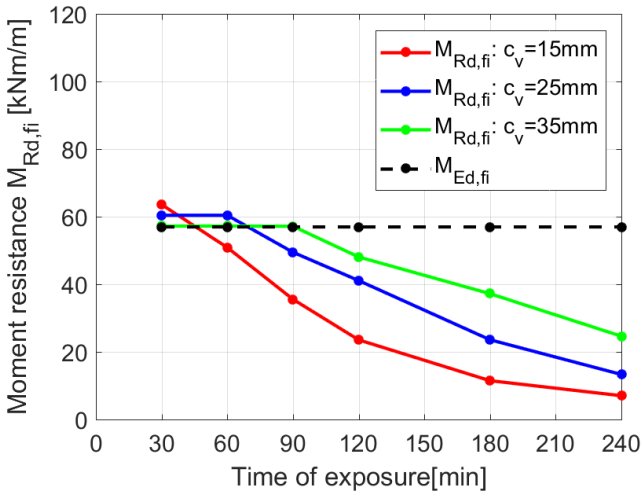

Fig. 24 Design section capacity of the slab in fire situation for standard ISO 834 fire model

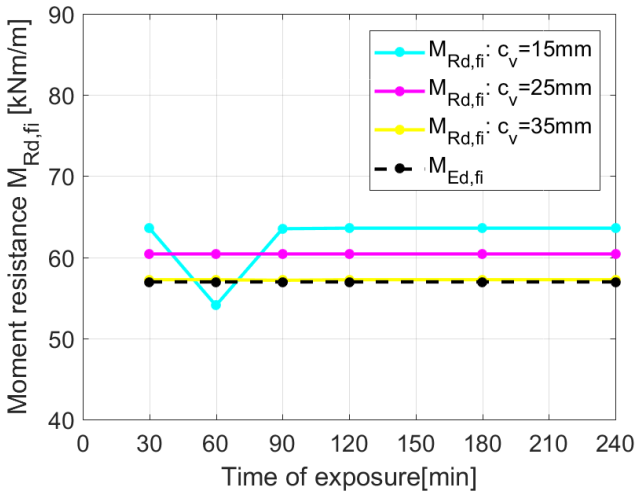

Fig. 25 Graphical interpretation of design flexural capacity of the slab in fire situation for parametric fire model-Ventilation controlled fire with opening factor O=0.05 $m^{1/2}$

fire design situation according to Eurocode 2. Adopting characteristical values of dead load and live load equal to 8.5 and 7.5 kN/m^2, respectively leads to the design fire load of 10.8 kN/m^2.

The results of the structural fire resistance are shown in the following tables.

The graphical interpretation of previous tabulated results is shown in Fig. 24.

It may be concluded that the proposed model of RC slab with concrete cover of 15 mm, 25 mm, and 35 mm, respectively possess fire resistance rating R30, R60, R90 per Eurocode provisions. The tabulated data from Eurocode 2, as an alternative approach for determining fire resistance, leads to the same results.

According to the provisions given in Eurocode 1, structural members have to satisfy certain conditions in terms of parametric fire exposure as well. The satisfactory level of fire resistance should be achieved during both the heating and cooling phase. Based on the temperature field from

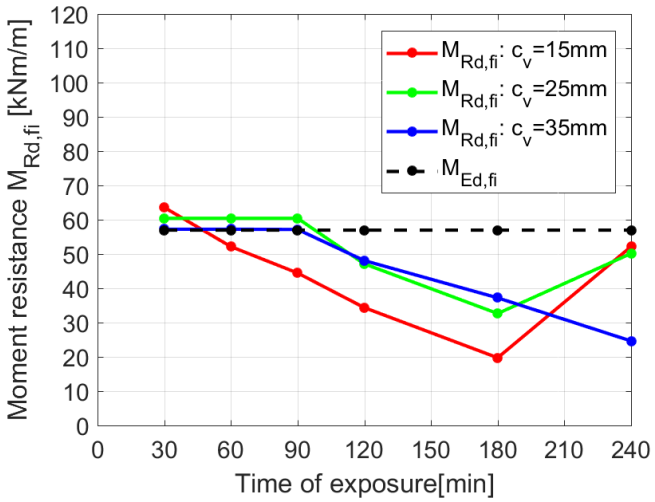

Fig. 26 Graphical interpretation of design flexural capacity of the slab in fire situation for parametric fire model-Ventilation controlled fire with opening factor O=0.10 $m^{1/2}$

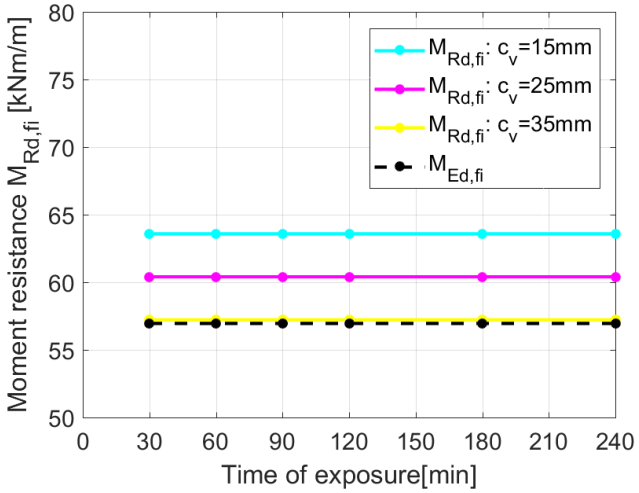

Fig. 27 Graphical interpretation of design flexural capacity of the slab in fire situation for parametric fire model-Fuel controlled fire with arbitrary opening factor and rate of fire growth (slow, medium or fast)

nonlinear transient heat analysis, the resistance of the critical cross-section assuming parametric fire exposures is shown below. Results corresponding to ventilation controlled fire are shown below:

In fuel controlled burning fire, the maximum temperature in reinforcement does not exceed 500°C. Thus reinforcement strength is not deteriorated by elevated temperatures enabling description of section capacity with just one time-independent curve regardless of both rates of fire growth and opening factors.

In addition to the previous approach, fully coupled thermo-mechanical analysis in finite element package DIANA FEA is carried out. Three-dimensional model discretized by solid elements representing concrete and grid reinforcement embedded in solid is presented (TNO DIANA: User's manual 2016).

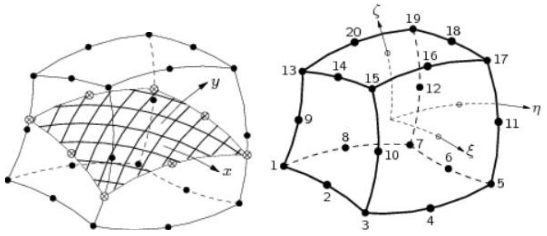

Fig. 28 Finite elements for modeling reinforcement and concrete

Table 6 Details of analyzed slab

Width (b)	1000 mm
Depth (H)	220 mm
Load intensity ($q_{Ed,fi}$)	10.8 kN/m^2
Yield stress of reinforcement (f_y)	500 N/mm^2
Concrete compressive strength (f_{ck})	25 N/mm^2
Reinforcement area - A_{st}	636 mm^2
Concrete cover (c_v)	15 mm
Fire exposure	Single-sided (bottom surface)
Fire model	Standard ISO 834 fire curve

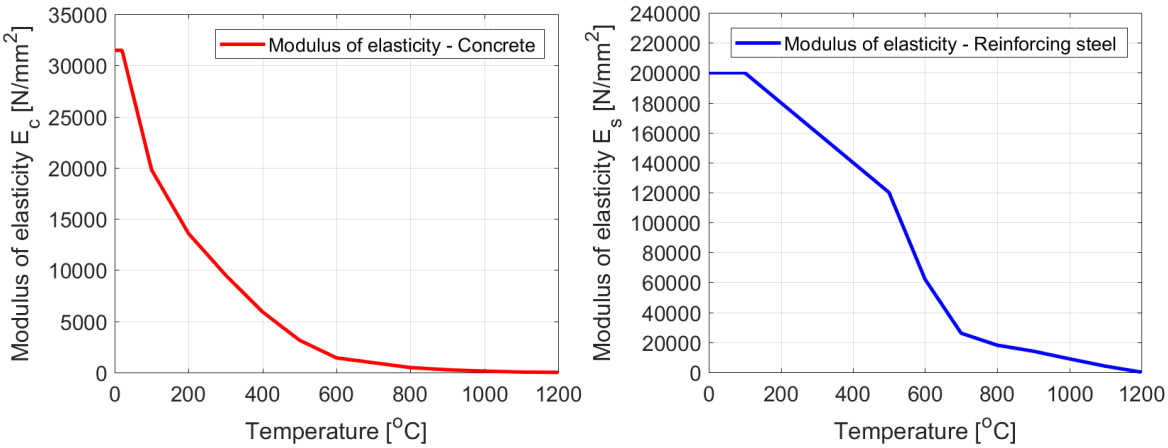

Fig. 29 Modulus of elasticity of concrete (left) and reinforcing steel (right) for calculation purposes

Both temperature-dependent strengths and modulus elasticity of constituent materials accounting for stiffness degradation during heating at elevated temperatures are used.

Reasonably, perfect adhesion without slip at interface reinforcement-concrete is assumed by ensuring reliable anchorage of reinforcement within the support zone (Khalaf *et al.* 2016, Pathisiri and Panedpojaman 2013).

The finite element mesh is divided by 11 layers of equal height along with mesh size in the layout of 250×250 mm. In order to reduce the computational cost, variable time step length is used leading to faster convergence. Thus time step length at the beginning of calculation accompanying by higher temperature rate is 60s, and 300 s thereafter remaining constant until the end of the

Table 7 Temperature field of the concrete slab

t=30 min	t=60 min
t=90 min	t=120 min
t=180 min	t=240 min

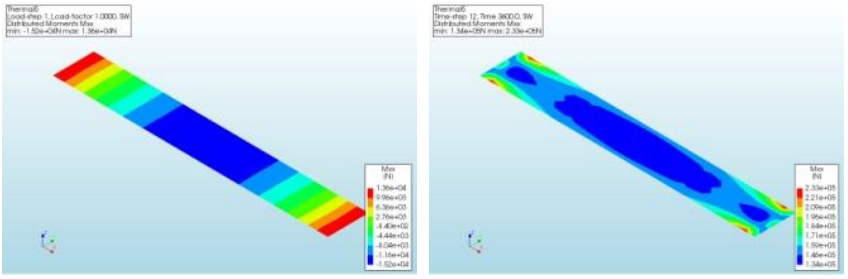

Fig. 30 Bending moments M_{xx} at time step t=0, t=60 min

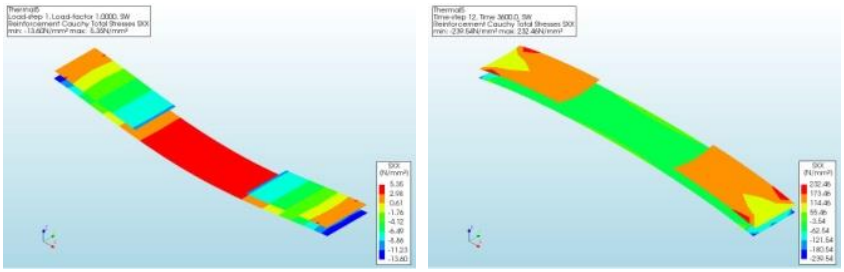

Fig. 31 Reinforcement stresses σ_{xx} at time step t=0, t=60 min

analysis. The results of thermal analysis in the form of temperature distribution across the slab are shown in Table 7.

One-dimensional heat transfer produces significant temperature gradients in bottom layers and heat fluxes related to them. Since the contribution of reinforcement on the temperature field is not largely observed in the proposed numerical model, its neglecting in previous approaches is justified. By decreasing thermal diffusivity during the elevated temperatures, changes in temperature field are less noticeable.

Results of mechanical analysis in the form of bending moments, reinforcement stresses and deflections are demonstrated.

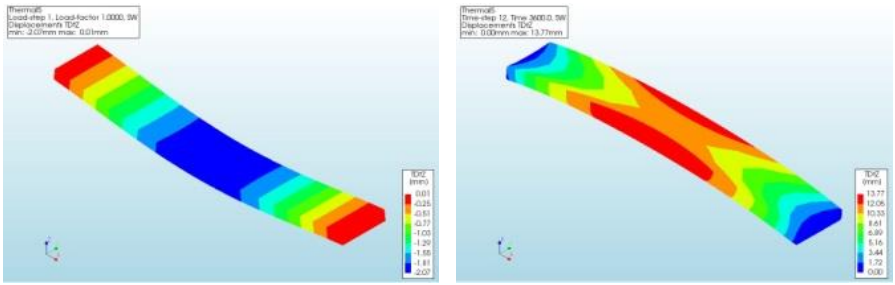

Fig. 32 Deflections at time step t=0, t=60 min

Bending moments for the proposed calculation model are no longer uniform since the curvature caused by heating of the tension zone of slab exists in both directions, unlike standard ambiental analysis. Increasing of the curvature is directly related to the temperature-dependent strengths of constituent materials leading not only in lower capacity but also in stiffness degradation. It can be observed in experimental tests (Guo and Shi 2011). Limitation of the excessive deformation closely linked with the stiffness degradation is one of the main functional requirements alongside requirements related to structural capacity in a fire design situation. The main advantage of this fully coupled numerical model compared to previous analysis is the capturing of the structural deflection accounting for highly non-linear stress-strain relationship and thermal properties of constituent materials.

4. Conclusions

In this paper, numerical coupled thermo-mechanical analysis accounting for nonlinear thermal characteristics is demonstrated. The following conclusion can be made:

- The nonlinear transient heat transfer model proposed in the study is capable to describe the development of temperature inside the structural element. The obtained results are perfectly fitted to those specified in Eurocode 2 implying the validation and verification of the model. The existing experimental and numerical study shows well agreement with the proposed results as well. Additionally, this makes the method greatly applicable to a huge range of problems in structural engineering which requires a comprehensive and thorough consideration of these problems.
- In the literature, it is possible to find results of heat transfer analysis in the form of temperature field just in certain cases concerning specific geometrical properties, thermal properties, heating regime, etc. This model uses the latter as a starting point of analysis making it really convenient dealing with the fire analysis. Furthermore, it can be easily modified in order to take account of two-dimensional heat transfer specific for beams and columns thereby including the most common structural concrete assembly in building construction.
- Regarding the mechanical part of structural fire analysis, it is shown that the concrete cover influences the results significantly. Insufficient value of concrete cover leads to reduced structural capacity in a fire design situation. The appropriate concrete cover is necessary not only for achieving a satisfactory level of fire resistance but also for durability demands applied to concrete structures. In that sense, two important aspects, durability and fire resistance, are coupled through just one parameter which underlines the significance of appropriate concrete cover thickness.

• Fully coupled one-way thermo-mechanical analysis, performed in finite element package DIANA FEA, has certain advantages compared to the Eurocode approach based on fire resistance rating. In both calculation approaches nonlinear thermal and mechanical properties are introduced which enable us to get insight into structural behavior during a fire. Using a fully coupled numerical approach, critical areas and structural weaknesses could be easily identified and could be performed appropriate measures in order to preserve structural integrity.

References

Allam, S.M., Elbakry, H.M.F. and Rabeai, A.G. (2013), "Behavior of one-way reinforced concrete slabs subjected to fire", *Alexandria Eng. J.*, **52**(4), 749-761. http://dx.doi.org/10.1016/j.aej.2013.09.004.

Balaji, A., Nagarajan, P. and Madhavan Pillai, T.M. (2016), "Predicting the response of reinforced concrete slab exposed to fire and validation with IS456 (2000) and Eurocode 2 (2004) provisions", *Alexandria Eng. J.*, **55**(3), 2699-2707. http://dx.doi.org/10.1016/j.aej.2016.06.005.

Bangash, M.Y.H., Al-Obaid, Y.F. and Bangash, F.N. (2014), *Fire Engineering of Structures-Analysis and Design*, Springer-Verlag Berlin Heidelberg, Germany.

Buchanan, A.H. and Abu, A.K. (2017), *Structural Design for Fire Safety*, 2nd Edition, John Wiley & Sons, Ltd.

Chandrasekaran, S. and Srivastava, G. (2018), *Design Aids of Offshore Structures under Special Environmental Loads Including Fire Resistance*, Springer, Singapore.

EN 1991-1 -2, Eurocode 1 (2002), Actions on Structures, Part 1.2: General Actions-Actions on Structures Exposed to Fire, Commission of the European Communities (CEN), Brussels, Belgium.

EN 1992-1 -2, Eurocode 2 (2004), Design of Concrete Structures, Part 1.2: General Rules-Structural Fire Design, Commission of the European Communities (CEN), Brussels, Belgium.

Ghaboussi, J. and Wu, X.S. (2017), *Numerical Methods in Computational Mechanics*, CRC Press, USA.

Guo, Z. and Shi, X. (2011), *Experiment and Calculation of Reinforced Concrete at Elevated Temperatures*, Elsevier, USA.

Huang, Z. (2010), "The behaviour of concrete slabs in fire", *Fire Saf. J.*, **45**(5), 271-282. https://doi.org/10.1016/j.firesaf.2010.05.001.

Ibrahimbegovic, A. (2009), *Nonlinear Solid Mechanics*, Springer, Dordrecht, Germany.

Ibrahimbegovic, A., Boulkertous, A., Davenne, L., Muhasilovic, M. and Pokrlic, A. (2010), "On modeling of fire resistance tests on concrete and reinforced-concrete structures", *Comput. Concrete*, **7**(4), 285-301. https://doi.org/10.12989/cac.2010.7.4.285.

Khalaf, J., Huang, Z. and Fan, M. (2016), "Analysis of bond-slip between concrete and steel bar in fire", *Comput. Struct.*, **162**, 1-15. https://doi.org/10.1016/j.compstruc.2015.09.011.

Logan, D.L. (2011), *A First Course in the Finite Element Method*, 4th Edition, CLEngineering, USA.

MATLAB (2017a), The MathWorks, Inc., Natick, Massachusetts, United States.

Ngo, M., Brancherie, D. and Ibrahimbegovic, A. (2014), "Softening behavior of quasi-brittle material under full thermo-mechanical coupling condition: Theoretical formulation and finite element implementation", *Comput. Meth. Appl. Mech. Eng.*, **281**, 1-28. http://dx.doi.org/10.1016/j.cma.2014.07.029.

Ngo, M., Ibrahimbegovic, A. and Brancherie, D. (2014), "Thermomechanics failure of RC composites: computational approach with enhanced beam model", *Coupl. Syst. Mech.,* **3**(1), 111-145. http://dx.doi.org/10.12989/csm.2014.3.1.111.

Ngo, V.M., Ibrahimbegovic, A. and Brancherie, D. (2013), "Model for localized failure with thermo-plastic coupling: Theoretical formulation and ED-FEM implementation", *Comput. Struct.*, **127**, 2-18. http://dx.doi.org/10.1016/j.compstruc.2012.12.013.

Pothisiri, T. and Panedpojaman, P. (2013), "Modeling of mechanical bond-slip for steel-reinforced concrete under thermal loads", *Eng. Struct.*, **48**, 497-507. https://doi.org/10.1016/j.engstruct.2012.10.015.

Purkiss, J.A. and Li, L. (2014), *Fire Safety Engineering: Design of Structures*, 3rd Edition, CRC Press, USA.

Sangluaia, C., Haridharan, M.K.., Natarajan, C. and Rajamaran, A. (2013), "Behaviour of Reinforced Concrete

Slab Subjected To Fire", *Int. J. Comput. Eng. Res.*, **3**(1), 195-206.
Suljevic, S., Medic, S. and Hrasnica, M. (2019), "Behavior of Concrete Structures Under the Action of Elevated Temperatures", *Advanced Technologies, Systems, and Applications IV-Proceedings of the International Symposium on Innovative and Interdisciplinary Applications of Advanced Technologies (IAT 2019)*, 250-262, Springer, Cham, Switzerland.
TNO DIANA (2016), User's Manual, DIANA FEA BV, Delft, The Netherlands.
Wickström, U. (2016), *Temperature Calculation in Fire Safety Engineering*, Springer, Switzerland.